Journal of Luminescence 161 (2015) 323–329

Contents lists available at ScienceDirect

Journal of Luminescence

journal homepage: www.elsevier.com/locate/jlumin

Temperature and host dependence of the transition interference between f–f and f–d transitions of Sm^{2+} in matlockites

Prodipta Pal [a,*], Hans Hagemann [a], Hans Bill [a], Jiahua Zhang [b]

[a] Département de Chimie Physique,Sciences II, Université de Genève, 30, Quai Ernest-Ansermet, CH-1211 Genève 4, Switzerland
[b] State Key Laboratory of Luminescence and Applications, Changchun Institute of Optics, Fine Mechanics and Physics, Chinese Academy of Sciences, 3888 Eastern South Lake Road, Changchun 130033, PR China

ARTICLE INFO

Article history:
Received 15 July 2014
Received in revised form
8 January 2015
Accepted 9 January 2015
Available online 21 January 2015

Keywords:
Fano resonance
Rare Earth
Sm^{2+}
Absorption

ABSTRACT

The absorption spectra of Sm^{2+} doped in MFX (M=Sr, Ba; X=Cl, Br) crystals were studied within the range of 20,000–35,000 cm^{-1} as a function of temperature and host. The absorption bands observed were described with a simple model developed by Wood and Kaiser using group theory. The temperature and host dependence on the $^7F_0 \rightarrow {}^5D_3$ Fano resonance lines were investigated. BaFCl:Sm^{2+} system showed a "normal" $^7F_0 \rightarrow {}^5D_3$ transition at 4 K in spite of similar crystal structure and absorption profile with other MFX hosts. New Fano resonances were observed in the absorption spectra at higher energies (23,000–25,000 cm^{-1}) for all MFX:Sm^{2+} systems at 4 K which persist up to room temperature. Preliminary energy level calculation showed that these resonance lines involve the interaction between higher excited ^5I_J states of $4f^6$ configuration and $4f^5 5d^1$ configuration.

1. Introduction

The interaction between discrete electronic levels and an overlapping continuum can give rise to interference effects producing characteristically asymmetric line shapes (antiresonances) of the transitions to the discrete levels. This effect for the first time was reported in He gas discharges (Beutler bands) and theoretically interpreted by Fano [1]. In the following these transitions will be designated (somewhat globally) as Fano lines. Subsequently, Fano lines were observed in the pre-dissociation region of molecular spectra [2,3]. Common to these systems was that both, the continuum and the discrete levels were of electronic nature. This quantum coherence was also observed in liquids [4] and solids. Solids containing Rare Earth (RE) or transition metal ions which have narrow transitions in their optical spectra may basically present Fano lines when the upper discrete level overlaps with a conduction band continuum or with broad vibronic bands of the same system [5–11]. A detailed study by Sturge et al. [7] on V^{2+} in crystals of $KMgF_3$ showed the presence of such line shapes, which were interpreted within the frame of the Fano theory. Fano resonances were previously observed [11] between f–f and f–d transitions in single crystals of SrFCl doped with Sm^{2+}. The observed $^7F_0 \rightarrow {}^5D_3$ transitions of the Sm^{2+} ion were anomalously strong and exhibited at 4 K a pronounced Fano double line profile which broadens with temperature but persists up to room temperature (RT).

Sm^{2+} doped in inorganic crystals is interesting for investigation as these systems have many exciting properties, such as room temperature hole burning [12] or as potential pressure sensors [13]. Recent observations showed that Sm^{3+}-doped in BaFCl nanocrystals presents efficient X-ray storage properties [14–16]. The storage mechanism is based on the reduction of Sm^{3+} to Sm^{2+} upon exposure to ionizing radiation [15]. Recently, photoluminescence of Sm^{2+}/Sm^{3+} doped in $Sr_4Al_{14}O_{25}$ was studied [17]; also the luminescence of Sm^{2+} was used to monitor pressure induced phase transitions in $BaBr_2$ [18].

Crystals within the matlockite (PbFCl-structure) family MFX (with M=Ca, Sr, Ba, Pb and X=Cl, Br, I) are an interesting subject of investigation for various reasons. Luminescence from BaFI and $BaFBr_{1-x}I_x$ crystals originates from self-trapped excitons [19]. Alkaline earth fluorohalides are useful for commercial applications (Eu-doped BaFBr for X-ray intensifying imaging plates or as storage phosphors [20]). They form solid solutions such as $SrFCl_xBr_{1-x}$ [21] which lead to an important inhomogeneous broadening of the Sm^{2+} emission [12,22], a condition for optical hole burning at high temperature.

The low temperature spectra of the BaFCl:Sm^{2+} system exhibit "normal" $^7F_0 \rightarrow {}^5D_3$ transitions in spite of the same crystal structure and a very similar f–d absorption spectrum with other matlockite hosts. It seemed therefore worthwhile to extend the Fano line investigation on Sm^{2+} to other matlockite hosts and to temperature dependence of these lines. In this paper we report the absorption spectra of Sm^{2+} in MFX host crystals. The absorption

* Corresponding author.
E-mail address: prodipta.pal08@gmail.com (P. Pal).

http://dx.doi.org/10.1016/j.jlumin.2015.01.030
0022-2313/

bands observed are described with a simple model developed by Wood and Kaiser [23]. The $^7F_0 \rightarrow {}^5D_3$ Fano resonance lines are studied as a function of host and temperature. New Fano resonance lines are observed as absorption dips in the spectra which involve the interaction with higher excited ^5L_J states of the $4f^6$ configuration.

2. Experimental

Crystalline samples were obtained by slow cooling of stoichiometric melts of the constituent halides (e.g. SrF_2+SrBr_2) under inert or 5%/95% H_2/N_2 atmosphere in graphite crucibles. Samarium was introduced as SmF_3 with a nominal concentration of 1% or less with respect to Sr or Ba. All MFX samples crystallize as thin platelets, and small single crystals were used for the luminescence experiments. Note that the MFX compounds (M=Ba, Sr and X=Cl, Br) are congruently melting, but potentially subject to the formation of solid solutions [24]. The purity of the samples was checked by inspecting the non-degenerate $^5D_0$–$^7F_0$ emission band, which can show small "satellite bands" when impurities are present close to the Sm^{2+} ion (for example Cl instead of Br), even in the second coordination sphere [22,25,26]. The emission spectra of our new samples are identical to those obtained in previous studies in our laboratory [21,22,24,25,27–30] with crystals grown under very strictly controlled conditions and characterized by X-ray diffraction and Raman spectroscopy as described in particular in Refs. [21,22,25].

The absorption measurements were performed with a double beam spectrometer (Varian Cary 5000) in the range of 200–600 nm with a resolution of 0.05 nm. The low temperature was achieved with a closed cycle cryostat capable of achieving temperatures down to 4 K (Janis-Sumitomo SHI-4.5), equipped with a programmable temperature controller (Lakeshore Model 331) allowing accurate control of the temperature. Spectra were recorded only in α geometry, except for SrFCl:Sm^{2+} where in addition also the α–π evolution of the absorption was obtained (E-field parallel-π geometry and perpendicular-α geometry, to the C_4 axis).

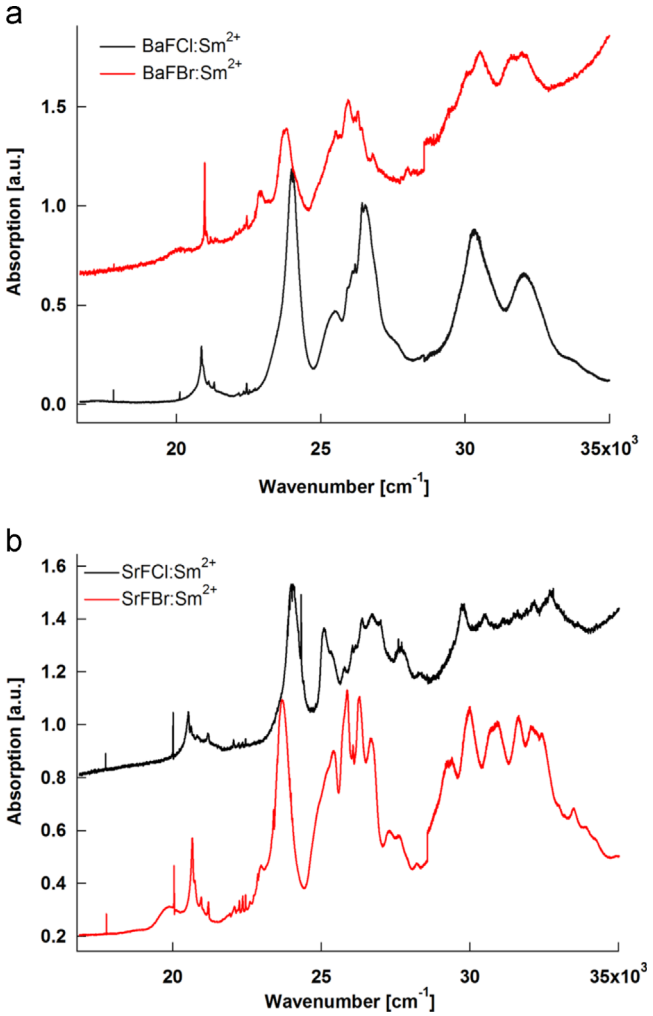

Fig. 1. Absorption spectra Sm^{2+} in (a) BaFCl, BaFBr and (b) SrFCl, SrFBr at 4 K.

3. Result and discussion

3.1. Absorption spectra of Sm^{2+} in MFX

The MFX:Sm^{2+} compounds present strong absorption bands between approximately 20,000 and 35,000 cm^{-1} [31,32]. The yellow coloration of matlockite compounds originates from this strong absorption. The absorption spectra of MFX:Sm^{2+} at 4 K are shown in Fig. 1. Note the intensity jump around 29,000 cm^{-1}. This is due to the change of grating of the instrument. All the compounds show similar overall spectra, although host dependent splitting, line position, relative intensities and detailed structure are present. Narrow f–f absorption lines are also observed. These include the ($^7F_0 \rightarrow {}^5D_2$) transition near 17800 cm^{-1}, the ($^7F_0 \rightarrow {}^5D_3$) Fano structure around 20,000 cm^{-1} and two quadruplets around 21,000 and 23,000 cm^{-1}, respectively. The superficial mutual similarity of the "glove" shapes and the quite small splitting between the "fingers" (Fig. 1) point to a rather similar static crystal field acting in the matlockites. The intra-atomic interactions are probably more important for the energy level structure than the crystal field effect.

A qualitative picture of the energy level structure underlying the absorption spectra can be constructed based on the arguments similar to the ones presented by Wood and Kaiser for MF_2:Sm^{2+} (M=Ca, Sr, Ba) [23]. The number and character of the energy levels are determined using group theory [33]. The 5d shell is considered as of strong field type as these orbitals extend far out towards the ligands and thereby experience strong perturbing crystal field effects. On the contrary, the 4f shell is of weak field type as these electrons are well screened by the outer ones.

This approximation allows a first assignments of the observed broad bands, however a formal assignment is much more complex, as has been demonstrated by the detailed analysis of the absorption spectrum of Sm^{2+} in $SrCl_2$ [34].

The site symmetry of Sm^{2+} is C_{4v} in the MFX host crystals. Eight anion neighbors form a square anti-prism. The Cl^- (or Br^-) square is capped by a fifth Cl^- (or Br^-) neighbor, leading to a global coordination number of 9. The bond angles C_4 axis–(M–X^-) (X=F, Cl or Br) of the square antiprism have values which depend on the host but are not far from half the tetrahedral angle (but are 0 resp. π for the two Cl^- or Br^- on the tetragonal axis). A quite strong host dependent crystal field (CF) results [35,36].

By descent in symmetry the (cubic) t_2 and e levels (e is lower) become B_2 (Γ_4) plus E (Γ_5) and A_1 (Γ_1) plus B_1 (Γ_3), respectively, (see Fig. 2). The two groups are separated by several thousand cm^{-1}. The Γ_3 (e) level is lowest. Including spin–orbit coupling results in 5 Kramers doublets transforming as 2 Γ_7, Γ_6 (t_2) and Γ_7, Γ_6 (e). When an electron is promoted from $4f^6$ to $4f^55d^1$ during the absorption process the remaining subshell ($4f^5$) has $^6H_{5/2}$ as the ground term which splits into 2 $\Gamma_7+\Gamma_6$ in C_{4v} symmetry.

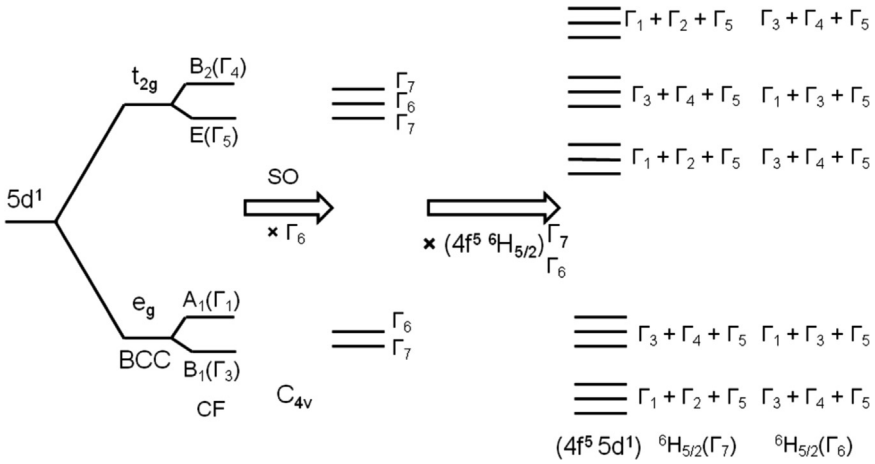

Fig. 2. Schematic energy level diagram for the $4f^5 5d^1$ configuration (CF=crystal field and SO=spin–orbit coupling).

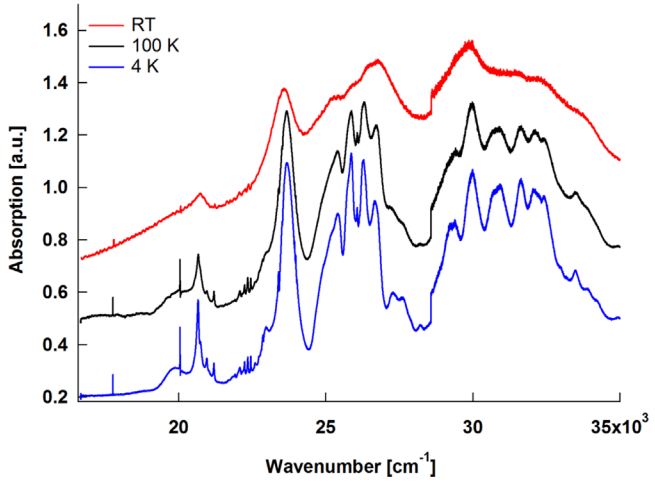

Fig. 3. Absorption spectra of SrFBr:Sm^{2+} at different temperatures.

Coupling Γ_7 to the Kramers doublets of the 5d manifold gives the species

$$(4f^{5}{}^{6}H_{5/2})\Gamma_7 \otimes (5d^1)\Gamma_7 = (4f^5 5d^1)\Gamma_1+\Gamma_2+\Gamma_5$$

And

$$(4f^{5}{}^{6}H_{5/2})\Gamma_7 \otimes (5d^1)\Gamma_6 = (4f^5 5d^1)\Gamma_3+\Gamma_4+\Gamma_5$$

for the e component. In a similar way from the t_2 component one can find $\Gamma_1+\Gamma_2+\Gamma_5$, $\Gamma_3+\Gamma_4+\Gamma_5$, $\Gamma_1+\Gamma_2+\Gamma_5$. Within the given approximations 15 energy levels (20 states) are obtained as shown in Fig. 2. Also given in the figure are the species obtained when $(4f^5\ {}^6H_{5/2})\ \Gamma_6$ coupled is coupled to the $(5d^1)$ manyfold. These will add additional structure to the five bands, where as the second Γ_7 would produce in first order "thickness" to the lines in the scale of Fig. 2. This energy level scheme qualitatively exhibits the main absorption bands and structures.

The absorption spectra as a function of temperature are given in Fig. 3 for the matlockite host SrFBr. The temperature effect on the absorption bands is similar for all four compounds under consideration. The width of the bands increases with temperature but the surface under the curve remains approximately constant – as expected for allowed transitions. The most pronounced changes are observed between RT and 100 K. The sharp structures disappeared heating from 100 K to RT.

The fine structure lines were observed between 20,000 and 23,000 cm^{-1} in all four host matrices. The identification of their origin is not immediate as their widths are in the tens of cm^{-1}, much larger than the $^7F_0 \rightarrow {}^5D_{0-2}$ transitions. But, the following results support the identification of the lines as f–f transitions of the Sm^{2+}. Their intensity is within experimental precision a constant multiple of the $^7F_0 \rightarrow {}^5D_2$ transition as verified in several samples obtained under widely different growth and treatment conditions and with a variety of concentrations of the samarium [37]. For the same reason they are excluded to arise from Sm^{3+} which might be present as an unwanted impurity i.e. it is very unlikely to find always the same ratios. Their assignment as single or multi-phonon structures of the lowest lying $4f^5 5d$ state can be dismissed as the splitting between the lines is much too large with respect to the phonon spectrum of the hosts. In addition, their temperature dependence between 4 and 200 K shows a very moderate increase in width. The main effect is a decrease in intensity, suggesting the action of the Huang–Rhys factor of a largely (zero-phonon) electronic transition – typical for f–f lines. Probably, the members within each quadruplet are crystal-field components of J multiplets of the higher excited states of $^5D_4$, $^5L_{6,7}$ and $^5G_{J(J=2-6)}$ of the $4f^6$ configuration [37]. Calculated free ion energy levels for SrFBr, BaFBr, SrFCl and BaFCl are tabulated in the Supplementary material.

3.2. $F_0 \rightarrow {}^5D_3$ Fano structures as a function of host and temperature

The absorption band located near 20,000 cm^{-1} is of particular interest with respect to interaction between discrete f–f and broad f–d continuum. The narrow transitions $^7F_0 \rightarrow {}^5D_3$ (around 20,000 cm^{-1}) are present in all four host crystals. Fig. 4 shows the absorption spectra of MFX:Sm^{2+} in the range between 17500 and 21,000 cm^{-1} at 4 K. A major difference between the chloride and bromide hosts can be found that is the presence of a separate wide Gaussian band in the latter two systems (BaFBr and SrFBr hosts) (see Fig. 4). This is indicated by arrows in Fig. 4. The wide Gaussian band merges with the 20,000 cm^{-1} quartet in the two chloride systems. Position and full width at half height of this Gaussian band was determined from the absorption spectrum which is given in Table 1.

The positions of the different peaks between 17500 and 22,500 cm^{-1} as a function of the host with sequence SrFCl, SrFBr, BaFCl, and BaFBr are shown in Fig. 5. Two important observations can be found from Fig. 5. There is a general shift to higher energies of the f–f transitions by going to the right in this figure.

On the other side, the f–d bands shift to higher energy from the bromide to the chloride for both strontium and barium compounds. The substitution of the bromine anion by chlorine introduces an upward shift of the band by approximately

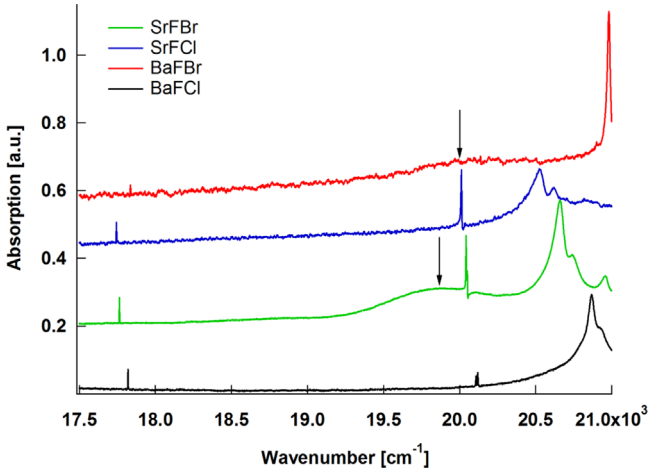

Fig. 4. Part of the absorption spectra of MFX:Sm^{2+} at 4 K between 17,500 and 21,000 cm^{-1}.

Table 1
Position and width of the lowest $4f^55d$ Gaussian band of Sm^{2+} in MFX hosts.

Host	Band position (cm^{-1})	FWHM (cm^{-1})
SrFCl	20,847	1010
SrFBr	20,003	1084
BaFCl	21,212	820
BaFBr	19,945	740

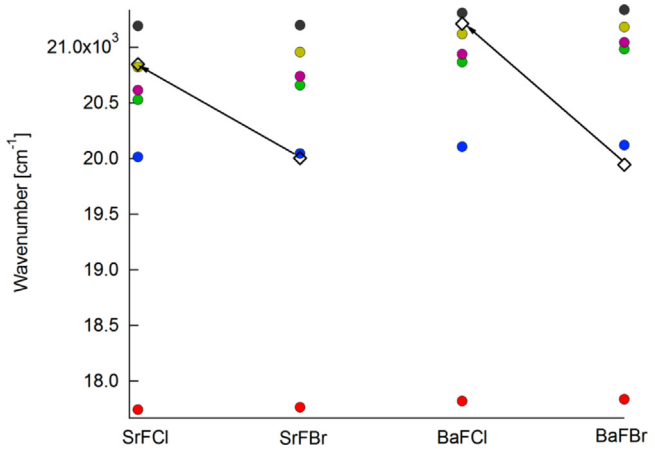

Fig. 5. Position of the absorption peaks as a function of the hosts for Sm^{2+} between 17,500 and 22,000 cm^{-1} at 4 K. The closed circles represent f–f transitions and open diamonds f–d transitions.

1150 cm^{-1}. It is of interest to compare the fluorescence quenching temperature T_q of the emissions from the $^5D_2$ level in the four hosts [28,37], where the following relation holds: T_q(BaFCl) > T_q(SrFCl) > T_q(BaFBr) > T_q(SrFBr). The quenching of these $^5D_2$ emissions takes place via thermal transfer to the lowest lying $4f^55d$ level [28,37]. Taking the energy difference between the center of the wide band and the $^5D_2$ line position, Δ(MFX)=E(band in MFX)–E($^5D_2$), one obtains: Δ(BaFCl) > Δ(SrFCl) > Δ(SrFBr) ≥ Δ(BaFBr). These facts concur with identifying the broad band as the lowest lying $4f^55d$ level. This band is further of importance for the lineshape of the $^7F_0 \rightarrow {}^5D_3$ transitions for the Fano interaction.

All four systems show at room temperature Fano profiles of these transitions – first identified in SrFCl:Sm^{2+} [11]. The $^5D_3$ term splits into $\Gamma_2+\Gamma_3+\Gamma_4+2\Gamma_5$ under C_{4v}. The symmetry allowed electric dipole transitions are thus to the $2\Gamma_5$ levels. The

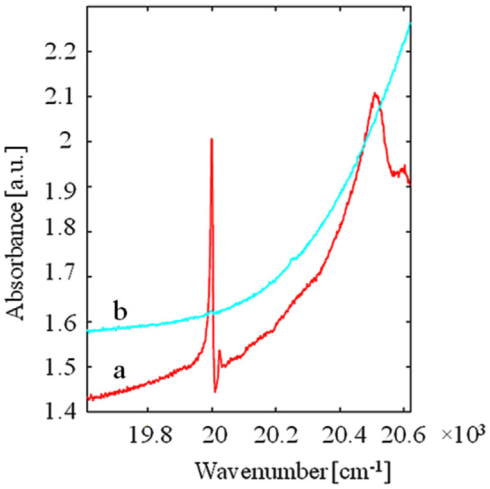

Fig. 6. Polarization of the $^7F_0 \rightarrow {}^5D_3$ transitions of SrFCl:Sm^{2+} at T=77 K. (a) $E_{incident} \perp C_4$, (b) $E_{incident} \| C_4$.

Table 2
Parameters of the fit of $^7F_0 \rightarrow {}^5D_3$ Fano structures presented in Fig. 7 using Eq. (1).

Hosts	T [K]	Γ_1	Γ_2	ν_1	ν_2	q_1	q_2
BaFCl	4.5	2.35	2.06	20,107	20,118	12.127	14.214
BaFBr	4.5	0.05	0.35	20,122	20,140	−1.025	0.247
SrFCl	4.5	6.48	2.55	20,015	20,036	−3.048	1.372
SrFBr	4.5	1.79	0.44	20,044	20,054	0.08	0.663
BaFCl	100	3.21	4.31	20,109	20,121	−11.544	−13.384
BaFBr	100	1.15	1.84	20,124	20,144	1.412	−2.945
SrFCl	100	7.81	3.57	20,014	20,035	−2.545	1.231
SrFBr	100	3.76	1.24	20,048	20,056	0.22	0.615
BaFCl	RT	9.95	6.8	20,113	20,128	−0.077	0.744
BaFBr	RT	7.41	9.95	20,125	20,146	−6.155	9.408
SrFCl	RT	14.92	4.65	20,026	20,049	−1.067	−0.222
SrFBr	RT	11.68	9.7	20,051	20,062	−1.168	0.916

absorption measurement under polarized light of SrFCl:Sm^{2+} at 77 K clearly demonstrated the symmetry assignment of the $^7F_0$ (A_1)→$^5D_3$ (E) transitions (see Fig. 6).

Fig. 7 present the experimental $^7F_0 \rightarrow {}^5D_3$ Fano structures of the four hosts recorded at 4 K, 100 K and RT. The black superposed curves were obtained by fitting Eq. (1) to the experimental curves [11].

$$\frac{K(\nu)}{K_0(\nu)} = (1-p) + p\frac{(\xi_1\xi_2 + \xi_1 q_2 + \xi_2 q_1)^2}{(\xi_1\xi_2)^2 + (\xi_1 + \xi_2)^2} \quad (1)$$

with

$$\xi_1 = \frac{\nu - \nu_1}{(\Gamma_1/2)},\ \xi_2 = \frac{\nu - \nu_2}{(\Gamma_2/2)}$$

where $K_0(\nu)$ is the absorption profile because of the continuum alone, parameters (ν_i, Γ_i, q_i) correspond to two discrete levels (i=1,2) and describe resonant frequency, linewidth, and asymmetry, respectively. The parameter P accounts for the additional background absorption if several continua are present. Programs developed under Matlab (versions R13 and R2011a), based on the Nelder–Mead minimization subroutines, were used. The parameters corresponding to the fit retained are given in Table 2.

Table 2 shows that with increasing temperature, the linewidths increase significantly, in particular for the Sr crystals. The differences of the broadening suggest that the coupling with phonons appears to be weaker for the Ba containing crystals. With increasing temperature, the positions of ν_1 and ν_2 shift to higher frequencies, due to the

thermal expansion of the crystals (opposite effect as the shift observed with pressure [27]).

BaFCl:Sm^{2+} shows at 4 K two "normal" lines corresponding to two unperturbed E terminal levels in absorption (see Fig. 8). Upon increasing the temperature to RT one observes, beginning around 100 K, the transformation into the Fano structure shown in Figs. 7 and 8, clearly visible in spite of considerable optical dephasing due to phonon relaxation at RT.

The other systems present Fano structures from 4 K up to RT as is most clearly seen for SrFCl in Fig. 7. Sm^{2+} in BaFCl has the highest energy of the 5d excited state (Table 1) among the investigated compounds. This is due to the lowest crystal field splitting as well as the lower nephelauxetic effect. As a result the essential differences between the two cases are the energy separation between the barycenter of $^5D_3$ and the center of the lowest-lying $4f^5$5d absorption band as well as the FWHH of this latter one. This splitting is $\approx 1020\ cm^{-1}$ in BaFCl:Sm^{2+} and is smaller by $\approx 280\ cm^{-1}$ in SrFCl:Sm^{2+}. In addition the FWHH of

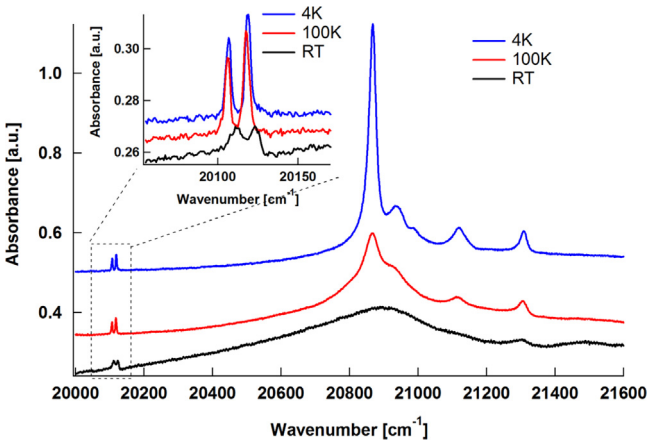

Fig. 8. Part of the absorption spectra of BaFCl:Sm^{2+} at 4 K, 100 K and RT. The inset shows the $^7F_0 \rightarrow {}^5D_3$ transition.

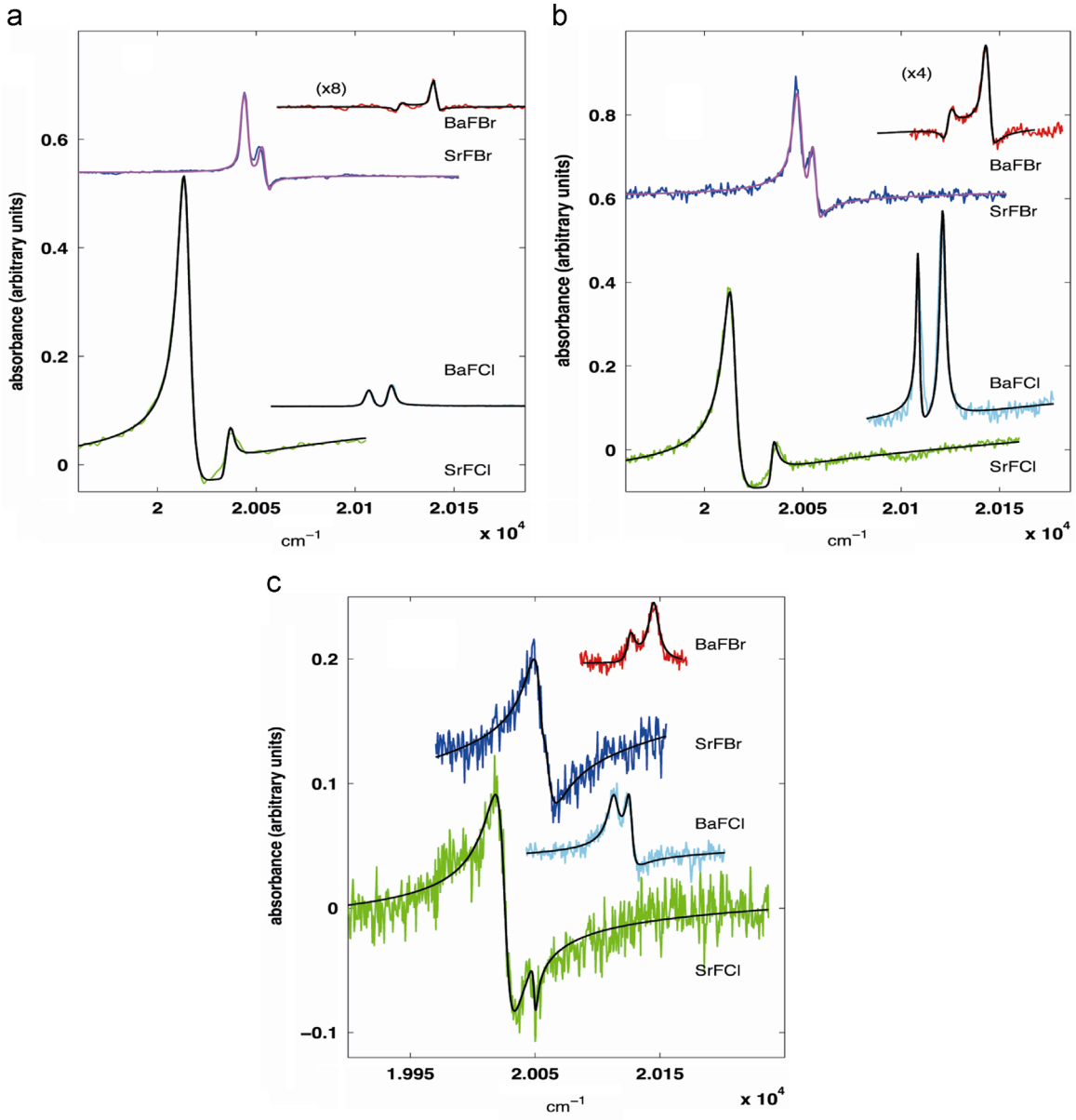

Fig. 7. $^7F_0(A_1) \rightarrow {}^5D_3(E)$ absorption lines of Sm^{2+} in BaFBr, SrFBr, SrFCl and BaFCl at 4 K (a), 100 K (b) and RT(c).

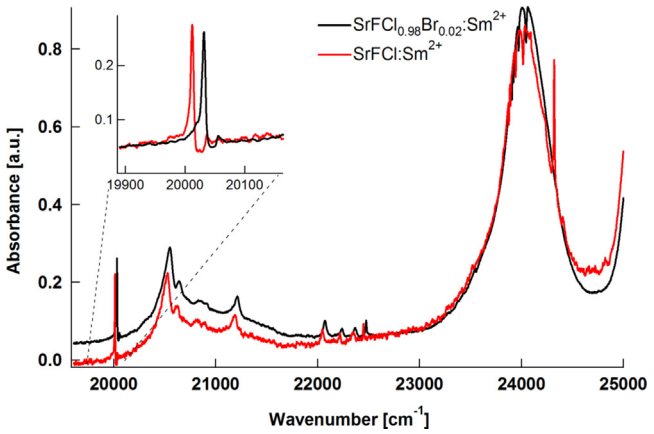

Fig. 9. Absorption spectra of pure SrFCl:Sm^{2+} and mixed $SrFCl_{0.98}Br_{0.02}$:Sm^{2+} at 4 K in the range of 19,500–25,000 cm^{-1}. The sharp band at ca 24,300 cm^{-1} in SrFCl (which is absent in mixed $SrFCl_{0.98}Br_{0.02}$:Sm^{2+}) is probably due to an impurity.

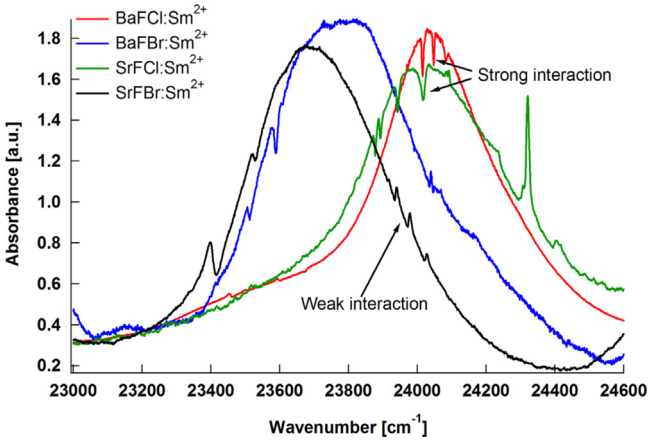

Fig. 10. Fano resonances observed for Sm^{2+} ion in MFX host involving ^5L_J levels at 4 K.

the fd band is ≈ 820 cm^{-1} in BaFCl and is ≈ 1010 cm^{-1} in SrFCl. Thus, the absence of Fano structure in BaFCl:Sm^{2+} at low temperature is indeed likely due to the very small overlap between the $^5D_3$ states and the Gaussian band, whereas in SrFCl a non-negligible overlap exists. This overlap increases for BaFCl with increasing temperature by a combination of line broadening and band shifts. An important parameter of the Fano model is indeed the density of states of the continuum at the energy of the localized levels as it determines the admixture between states [1]. For the same reason the $^5D_{0-2}$ lines do not show Fano profiles as they are ≥ 5000 cm^{-1} below the Gaussian bands. Additional information was gained from experiments done on mixed crystals of composition $SrFCl_xBr_{1-x}$:Sm^{2+} ($0.85 \le x \le 1$). One example of the pure SrFCl and mixed compound's absorption spectra is shown in Fig. 9. The different clusters which exist in these systems [25] showed Fano lines very similar to the pure SrFCl case. No differences in the interaction parameters of Eq. (1) were found [37]. The Gaussian band was observed to present a wider FWHH with practically the same center frequency. In spite of small shifts in the position of the Fano profiles this fact provided for non-negligible overlap for all of the possible local clusters.

3.3. Fano resonances at higher energy

The new Fano antiresonance lines were observed for all the four compounds between 23,000 and 25,000 cm^{-1} as absorption dips in the spectra (see Fig. 10). Similar dips were found for Eu^{2+} doped compounds in the excitation spectra due to interaction between ^6I_J of $4f^7$ configuration and $4f^65d^1$ configuration [9] and V^{2+} [7], Cr^{3+} [10] d^3 transition metal based on the interaction between the intra-t_2^3 levels (^2E, $^2T_1$, $^2T_2$) and the t^2e levels ($^4T_2$, $^4T_1$). The Fano antiresonance lines observed at higher energies for Sm^{2+} are much more pronounced than observed before for the rare-earth doped compounds. These Fano antiresonance lines observed at 4 K persist up to RT with the broadening of the dips in the absorption peak. Stronger interactions of higher excited ^5L_J levels of $4f^6$ configuration with $4f^55d^1$ configuration are present for the chloride compounds and weaker interactions for the bromide compounds (see Fig. 10). In the case of chloride compounds, the strong dips are observed close to the maximum of the broad fd absorption band, while for the bromide compounds, the Fano interactions appear closer to the tail of this broad band. Preliminary energy level calculations of Sm^{2+} in these four host materials show that higher excited states $^5L_{J(J=8-10)}$ of $4f^6$ configuration are involved for these resonances [37]. This observation needs further theoretical analysis to understand the origin of the antiresonance dips in the absorption spectra.

4. Conclusions

The strong broad absorption bands of Sm^{2+} in matlockite host crystals originate from the $^7F_0$ level (ground state) of the $4f^6$ configuration to the $4f^55d^1$ configuration. They are described qualitatively taking into account the strong ligand field for 5d orbitals and weak field for the 4f orbitals. The group theoretical analysis suggests Γ_6 as the lowest state of $4f^55d^1$ $^6H_{5/2}$.

The $^7F_0$ (A_1)→$^5D_3$ (E) Fano resonance lines of Sm^{2+} are studied as a function of host and temperature. BaFCl:Sm^{2+} shows a different behavior than the other hosts at low temperatures as it forms two practically normal $^7F_0$ (A_1)→$^5D_3$ (E) absorption bands. This is due to the negligible overlap between the $^5D_3$ (E) levels and broad $4f^55d^1$ band. At higher temperature the overlap becomes stronger, which shows Fano resonance lines similar to the other MFX host crystals.

New Fano resonance lines are observed as absorption dips at broad fd absorption band between 23,000 and 25,000 cm^{-1} which originates from $^5L_{J(J=8-10)}$ levels of $4f^6$ configurations.

Acknowledgment

This work is supported by the Swiss National Science Foundation (project no. 126653). The authors thank Prof. R. Jaaniso for former work on Fano resonances in SrFCl:Sm^{2+}.

Appendix A. Supporting information

Supplementary data associated with this article can be found in the online version at http://dx.doi.org/10.1016/j.jlumin.2015.01.030.

References

[1] U. Fano, Phys. Rev. 124 (1961) 1866.
[2] P. Lambropoulos, P. Zoller, Phys. Rev. A 24 (1981) 379.
[3] K. Rzazewski, J.H. Eberly, Phys. Rev. Lett. 47 (1981) 408.
[4] A. Shibatani, Y. Toyozawa, J. Phys. Soc. Jpn. 25 (1968) 335.
[5] M. Taylor, Phys. Rev. Lett. 23 (1969) 405.
[6] V. Arkangel'skaya, P.P. Feofilov, Opt. Spectrosc. 28 (1970) 657.
[7] M.D. Sturge, H.J. Guggenheim, M.H.L. Pryce, Phys. Rev. B 2 (1970) 2459.
[8] M.S. Skolnick, P.R. Tapster, P.J. Dean, R.G. Humphreys, B. Cockayne, W.R. MacEwan, J.M. Noras, J. Phys. C: Solid State. 15 (1982) 3333.
[9] A. Meijerink, G. Blasse, Phys. Rev. B 40 (1989) 7288.
[10] A. Lempicki, L. Andrews, S.J. Nettel, B.C. McCollum, Phys. Rev. Lett. 44 (1980) 1324.
[11] R. Jaaniso, H. Bill, Phys. Rev. B 44 (1991) 2389.
[12] R. Jaaniso, H. Bill, Europhys. Lett. 16 (1991) 569.

[13] Y.R. Shen, T. Gregorian, W. Holzapfel, High Press. Res. 7 (1991) 73.
[14] Z. Liu, T. Massil, H. Riesen, Phys. Procedia 3 (2010) 1539.
[15] Z. Liu, M. Stevens-Kalceff, H. Riesen, J. Phys. Chem. C 116 (2012) 8322.
[16] H. Riesen, W.A. Kaczmarek, Inorg. Chem. 46 (2007) 7235.
[17] S. Sakirzanovas, A. Katelnikovas, D. Dutczak, A. Kareiva, T. Jüstel, J. Lumin. 131 (2011) 2255.
[18] M.C. Wiegand, W. Sievers, J.K.N. Lindner, Th. Tröster, S. Schweizer, J. Lumin. 131 (2011) 2400.
[19] A. Ohnishi, K. Kan'no, Phys. Status Solidi B 245 (2008) 2815.
[20] K. Takahashi, J. Lumin. 100 (2002) 307.
[21] R. Jaaniso, H. Hagemann, F. Kubel, H. Bill, Chimia 46 (1992) 133.
[22] H. Bill, R. Jaaniso, H. Hagemann, D. Lovy, A. Monnier, M. Schnieper, Opt. Eng. 34 (1995) 2333.
[23] D.L. Wood, W. Kaiser, Phys. Rev. 126 (1962) 2079.
[24] H. Hagemann, P. Tissot, D. Lovy, F. Kubel, H. Bill, J. Therm. Anal. Calorim. 57 (1999) 193.
[25] R. Jaaniso, H. Hagemann, H. Bill, J. Chem. Phys. 101 (1994) 10323.
[26] F. Kubel, H. Hagemann, H. Bill, Mater. Res. Bull. 30 (4) (1995) 405.
[27] P. Pal, T. Penhouet, V. D'Anna, H. Hagemann, J. Lumin. 134 (2013) 678.
[28] P. Pal, T. Penhouet, V. D'Anna, H. Hagemann, J. Lumin. 142 (2013) 66.
[29] P. Pal, H. Hagemann, in: Proceedings of the Seventh International Conference on f Elements, Terrae Rarae, Gerd Meyer Ed., 06, (2009), pp. 1.
[30] T. Penhouet, H. Hagemann, J. Alloy. Compd. 451 (2008) 74.
[31] Y.R. Shen, W.B. Holzapfel, Phys. Rev. B 51 (1995) 6127.
[32] Z. Kiss, H. Weakliem, Phys. Rev. Lett. 15 (1965) 457.
[33] J.A. Salthouse, M.J. Ware, Point Group Character Tables and Related Data, Cambridge University Press, 1972.
[34] M. Karbowiak, A. Urbanowicz, M. Reid, Phys. Rev. B 76 (2007) 115125.
[35] H.P. Beck, J. Solid State Chem. 17 (1976) 275.
[36] D. Nicollin, H. Bill, Solid State Commun. 20 (1976) 135.
[37] P. Pal, Photophysical properties of samarium (II) doped in inorganic crystals: effect of chemical environment, external pressure and temperature (Ph. D. Thesis), Université de Genève, 2012 ⟨http://archive-ouverte.unige.ch/unige:24868⟩.